

Enhanced pairing mechanism in Cuprate-type crystals

Maximilian Duell,^a Christian Hainzl,^b and Eman Hamza^c

Mathematisches Institut, Ludwig-Maximilians-Universität München, 80333 Munich, Germany

Using a BCS mean-field approach, we show how the interplay between low-momentum optical phonons and Jahn-Teller-type lattice distortions can open an attractive channel that allows the formation of pairs with the corresponding density exhibiting characteristic features of a pair-density wave (PDW). We demonstrate this numerically on a copper-oxide type lattice.

While the pairing mechanism in conventional superconductors has long been well understood, the situation for cuprate superconductors is still controversial and unexplained thirty-five years after their discovery. Although the traditional phonon-mediated BCS pairing mechanism has been largely ruled out as the main cause of high-temperature superconductivity, several experimental groups, e.g. [1, 2], reported observations of sufficiently strong interactions between certain optical modes and doped charge carriers. A number of recent experiments [3, 4] further suggest a pronounced correlation between the superconducting gap and the strength of electron-phonon coupling at small momentum transfer [5, 6]. Bednorz and Müller [7] were motivated in their search for new superconducting materials by the idea that lattice distortions in the sense of dynamic Jahn-Teller polarons could be the novel glue for electron pairing, much stronger than the conventional BCS pairing mechanism [8, 9]. In light of their sensational success, it seems perfectly reasonable to assume that this fundamental discovery of copper oxide superconductors was no coincidence, but rather confirmation of the fact that strong dynamic lattice distortions are required to achieve high values of T_c . Such dynamic distortions undoubtedly seem to play a role in cuprates [10, 11].

The aim of the present work is to present a novel pairing mechanism driven by a synergy of Jahn-Teller type crystal lattice deformations and optical phonon vibrations. By conventional wisdom the standard pairing cannot contribute to the large critical temperatures as observed in copper oxides. With this in mind we restrict ourselves instead to pairs \mathbf{k}, \mathbf{k}' such that $\frac{|\mathbf{k}-\mathbf{k}'|}{|\mathbf{k}_F|} \ll 1$ with both momenta close to the Fermi sea.

In a recent paper, one of the authors (C.H.) and M. Loss [12] pointed out that for interactions more general than depending only on relative distance, arbitrary electron pairs with momenta \mathbf{k}, \mathbf{k}' and equal energy $\varepsilon(\mathbf{k}) = \varepsilon(\mathbf{k}')$ can lead to instability of the Fermi sea. For reasons of simplicity we shall restrict ourselves here to pairs with equal momentum and opposite spin, and we will see that that in this case a remarkable explicitly solvable model is obtained. Therein the pair-forming effective interactions

result from the above mentioned combination of optical phonon interactions and lattice deformations. Interestingly, once the effective interaction has been determined, the corresponding gap equation has a much simpler structure compared to the conventional case. Most notably, the critical temperature depends linearly on the interaction strength.

Let us now become more concrete. We consider a diatomic copper oxide lattice (see Figure 1). Using Wegner flow methods [13, 14], we obtain an effective interaction between charge carriers, similar to the earlier derivations of Fröhlich [15], and Bardeen-Pines [16]. The exact form of the effective interaction depends on the details of the associated Bloch functions and hence on the details of the lattice geometry.

Consequently, we apply the BCS approximation to the resulting Hamiltonian and investigate the possibility of correlated pairs due to the instability of the Fermi sea. In other words, we consider the non-interacting Fermi gas as the parent compound for the superconducting behavior, with the chemical potential $\varepsilon(\mathbf{k}_F)$ playing the role of the doping parameter. Once we obtain an effective interaction, we consider the resulting BCS gap equation, which now takes the following simplified form

$$\left(\frac{\sqrt{(\varepsilon(\mathbf{k}) - \varepsilon(\mathbf{k}_F))^2 + |\Delta(\mathbf{k})|^2}}{\tanh\left(\frac{\sqrt{(\varepsilon(\mathbf{k}) - \varepsilon(\mathbf{k}_F))^2 + |\Delta(\mathbf{k})|^2}}{2T}\right)} + \frac{V(\mathbf{k})}{2} \right) \Delta(\mathbf{k}) = 0, \quad (1)$$

where \mathbf{k} is the crystal momentum, \mathbf{k}_F the Fermi momentum and V is the effective interaction, with attractive component $V \leq 0$. On the one hand, our simplifications lead to the nice equation (1), but on the other hand they have unfortunately removed the phase dependence, since the solutions of (1) are uniquely determined only up to an arbitrary phase $e^{i\theta(\mathbf{k})} \Delta(\mathbf{k})$. For this reason, our numerical solutions of the gap equation is only concerned with the absolute values of Δ . Further, it is important to emphasize the following; if the crystal lattice is perfectly symmetrical, then the effective interaction $V(\mathbf{k})$ vanishes identically. However, Jahn-Teller-type lattice distortions, which form dynamically in presence of charge carriers, allow non-vanishing interactions $V(\mathbf{k})$, which in turn open attractive channels for Cooper pairing. We present an example of such an interaction in Section III. The solution $\Delta(\mathbf{k})$ in (1) is automatically concentrated near the Fermi sea, as seen in Figure 5. The corresponding critical

^aElectronic address: duell@math.lmu.de

^bElectronic address: hainzl@math.lmu.de

^cElectronic address: hamza@math.lmu.de

pairing temperature T^* has the simple form

$$T^* = -\frac{V(\mathbf{k}_F)}{4}. \quad (2)$$

Let us emphasize that the magnitude of the interaction $V(\mathbf{k}_F)$ depends significantly on the strength of the coupling of charge carriers to the lattice, which according to (2) determines the temperature T^* , below which the BCS approach predicts the occurrence of correlated pairs. This is in line with the original insightful heuristics used by Bednorz and Müller in their successful searches for superconducting materials.

We propose the following interpretation of our work for copper oxide materials: Since we neglect the strong Coulomb repulsion among electrons and use the BCS mean-field approach, our analysis cannot be directly applied to the occurrence of superconductivity itself, but it could well describe the pseudo-gap (PG), where T^* is the corresponding critical temperature. If the chemical potential $\varepsilon(\mathbf{k}_F)$ models the amount of doping, then the phase diagram of T^* can be explained by the fact that the coupling strength between charge carriers, e.g. electrons, and the crystal lattice depends on the velocity of the charge carriers. The faster the particles are, the smaller the effect of deformation and the weaker the effective coupling potential. This is also an apparent explanation for the disappearance of superconductivity above certain doping levels. Namely, we propose that the PG phase is caused by BCS-like pairing, but with pairs with momenta $\frac{|\mathbf{k}-\mathbf{k}'|}{|\mathbf{k}_F|} \ll 1$ that are close to each other. These pairs however do not necessarily allow for macroscopic coherence, i.e. long range order.

The appearance of pairings with finite center-of-mass momentum was suggested in the sixties by Fulde-Ferrell [17] and by Larkin-Ovchinnikov [18, 19] independently and is nowadays referred to as FFLO phases. The pairs we study here are of a different nature since their total momentum varies along the Fermi surface. However, the form of these pairs naturally implies the existence of a pair density wave (PDW), even though the pairing mechanism we propose here is clearly different than the one usually discussed in the literature, see e.g [20, 21].

The paper is organized as follows: in the next section, we discuss the electron-phonon coupling in CuO_2 and the resulting effective electron-electron interaction. The well-known derivations for these results are briefly outlined in the Appendix. Section II is dedicated to the BCS gap equation arising from the presence of equal momenta electron pairs. In Section III we calculate distortion effects on the effective electron-electron interaction in a tight-binding model. Finally, in Section IV we describe numerical results showing that such Jahn-Teller type distortion can give rise to non-zero electron-phonon coupling between pairs of electrons with equal momenta and opposite spin and we discuss the resulting gap function and pair wave densities.

I. EFFECTIVE ELECTRON-ELECTRON INTERACTION IN CuO_2

As an example of a system which allows for the above described pairing mechanism, we consider a planar CuO_2 lattice with volume Ω and square primitive cells composed of one Copper atom and two Oxygen atoms per unit cell, see Figure 1.

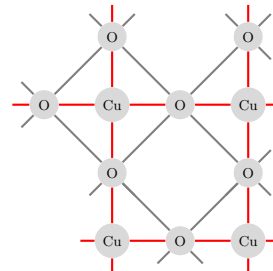


FIG. 1: Two dimensional CuO_2 cubic lattice

We are mainly interested in the interaction between Bloch electrons and lattice phonons. Starting with the standard many-body Hamiltonian, the renormalization flow of Wegner [13, 14] yields an effective electron model where the electron-phonon interaction is replaced by an effective electron-electron interaction mediated by the phonons. The leading-order effective Hamiltonian has the general form

$$H_{\text{el}} = \sum_{\mathbf{k}, n, \sigma} \varepsilon_n(\mathbf{k}) c_{n\mathbf{k}\sigma}^\dagger c_{n\mathbf{k}\sigma} + \sum_{\substack{\mathbf{k}n\sigma, \mathbf{k}'m\sigma' \\ \mathbf{q}n'm'\mathbf{G}\mathbf{G}'}} V_{\sigma\sigma'}^{nn'mm'}(\mathbf{k}, \mathbf{k}', \mathbf{G}, \mathbf{G}', \mathbf{q}) \cdot c_{n'\mathbf{k}+\mathbf{q}+\mathbf{G}\sigma'}^\dagger c_{m'\mathbf{k}'-\mathbf{q}+\mathbf{G}'\sigma'} c_{m\mathbf{k}\sigma'} c_{n\mathbf{k}\sigma}, \quad (3)$$

where $\varepsilon(\mathbf{k})$ is the electronic dispersion relation, σ, σ' the electronic spins and V the effective attractive interaction between electrons with momenta \mathbf{k}, \mathbf{k}' through a phonon with momentum \mathbf{q} and umklapp vectors \mathbf{G}, \mathbf{G}' . It is worth noting that the Wagner flow method has been previously used to study electron-phonon interactions in other models, see e.g. [22].

We are interested in possible pairing mechanism of electrons with momenta \mathbf{k}, \mathbf{k}' , with $\frac{|\mathbf{k}-\mathbf{k}'|}{|\mathbf{k}_F|} \ll 1$ and both momenta are close to the Fermi sea with an effective interaction mediated by phonons with low momenta \mathbf{q} . However, in order to obtain an explicitly solvable model, we further simplify this model by concentrating on pairs with equal momenta. Thereby (3) can be restricted to $\mathbf{k} = \mathbf{k}'$, and $\mathbf{k} + \mathbf{q} + \mathbf{G} = \mathbf{k}' - \mathbf{q} + \mathbf{G}'$. Solving for the phonon momentum gives $\mathbf{q} = \frac{\mathbf{G}' - \mathbf{G}}{2}$. In the first Brillouin zone (FBZ) this has the trivial solution $\mathbf{q} = \mathbf{0}$ and four further distinct solutions on the boundary, $\mathbf{q} = (\pi, 0)$, $(0, \pi)$, and $(\pi, \pm\pi)$, where the lattice constant $a = 1$ in natural units.

Since we are interested in small momentum transfers, we focus on the case of $\mathbf{q} = \mathbf{0}$. It cannot be overemphasized that this should be considered as an approximation that captures the essential physical mechanism, whereas in an actual physical system any sufficiently small momentum transfer \mathbf{q} , and likewise any Bloch momentum pairs \mathbf{k}, \mathbf{k}' that are sufficiently close to each other on the scale of the Fermi momentum \mathbf{k}_F , i.e. $\frac{|\mathbf{k}-\mathbf{k}'|}{|\mathbf{k}_F|} \ll 1$, can contribute.

Neglecting electron-electron Coulomb interactions, we obtain a reduced effective Hamiltonian of the form

$$H_{\text{eff}} = \sum_{\mathbf{k}\sigma} \varepsilon(\mathbf{k}) c_{\mathbf{k}\sigma}^\dagger c_{\mathbf{k}\sigma} + \sum_{\mathbf{k}, \sigma, \sigma'} V(\mathbf{k}) c_{\mathbf{k}\sigma}^\dagger c_{\mathbf{k}\sigma'}^\dagger c_{\mathbf{k}\sigma'} c_{\mathbf{k}\sigma}. \quad (4)$$

In the following sections, we explore the possible pair formation within this toy model. In the Appendix we briefly outline the standard derivation of the effective electron-electron interaction (3) in the *rigid-ion* approximation. There one obtains for (4) that

$$V(\mathbf{k}) = - \sum_{\lambda} \frac{1}{\omega_{\lambda}(\mathbf{0})} |D_{\lambda}(\mathbf{k})|^2. \quad (5)$$

where $\omega_{\lambda}(\mathbf{0})$ is the optical phonon energy at zero momentum, and the electron-phonon coupling $D_{\lambda}(\mathbf{k})$ is given by

$$D_{\lambda}(\mathbf{k}) = i \sqrt{\frac{\hbar N_{\text{cell}}^3}{2\omega_{\lambda}(\mathbf{0})\Omega^4}} \sum_{\tau} \sum_{\tilde{\mathbf{G}} \in \text{RL}} \mathbf{e}_{\lambda, \tau}(\mathbf{0}) \cdot \tilde{\mathbf{G}} \frac{\hat{v}_{\text{ei}}^{\tau}(\tilde{\mathbf{G}})}{\sqrt{M_{\tau}}} \cdot \int_{\text{cell}} d^2r e^{i\tilde{\mathbf{G}} \cdot \mathbf{r}} |u_{\mathbf{k}}(\mathbf{r})|^2, \quad (6)$$

Here N_{cell} is the number of primitive cells in a lattice of volume Ω , τ runs over the atomic basis, M_{τ} the mass of the τ ion and $\hat{v}_{\text{ei}}^{\tau}$ the Fourier transform of the *spin-independent* electron-ion potential, defined as

$$\hat{v}_{\text{ei}}^{\tau}(\mathbf{Q}) = \int_{\Omega} d^2r v_{\text{ei}}^{\tau}(\mathbf{r}) e^{-i\mathbf{Q} \cdot \mathbf{r}} \quad (7)$$

Moreover, $e_{\lambda, \tau}$ are the polarization vectors, while $u_{\mathbf{k}}$ are the lattice periodic electronic wave functions and the integral is over the volume of the unit cell. See the Appendix for details.

II. BCS APPROACH TO EQUAL MOMENTUM PAIRING

We would like to emphasize that, as pointed out in [12], any pairing, \mathbf{k}, \mathbf{k}' with $\varepsilon(\mathbf{k}) = \varepsilon(\mathbf{k}')$, can lead to the instability of the Fermi sea. Choosing equal momentum pairing allows us to obtain a gap equation that depends on only one momentum. Let us now apply the usual BCS mean-field approach to (4), with the gap function for equal momentum pairing defined by

$$\Delta(\mathbf{k}) = V(\mathbf{k}) \langle c_{\mathbf{k}\downarrow} c_{\mathbf{k}\uparrow} \rangle. \quad (8)$$

Following standard arguments we obtain the gap equation

$$\left(\frac{E_{\Delta}(\mathbf{k})}{\tanh\left(\frac{E_{\Delta}(\mathbf{k})}{2T}\right)} + \frac{V(\mathbf{k})}{2} \right) \Delta(\mathbf{k}) = 0, \quad (9)$$

with

$$E_{\Delta}(\mathbf{k}) = \sqrt{(\varepsilon(\mathbf{k}) - \varepsilon(\mathbf{k}_F))^2 + |\Delta(\mathbf{k})|^2}. \quad (10)$$

The corresponding equation for the critical temperature T^* ,

$$\frac{E_0(\mathbf{k}_F)}{\tanh\left(\frac{E_0(\mathbf{k}_F)}{2T^*}\right)} = -\frac{V(\mathbf{k}_F)}{2}, \quad (11)$$

reduces to the particularly simple relation

$$T^* = -\frac{V(\mathbf{k}_F)}{4}. \quad (12)$$

The linear dependence on the coupling distinguishes this type of pairing from conventional superconductors. Here, the critical pairing temperature T^* is directly determined by the strength of the lattice deformation. A particular weakness of our approach is the loss of phase dependence, since the solution of (9) is determined only up to an arbitrary phase function $e^{i\theta(\mathbf{k})}$.

It should be mentioned that in recent years the mathematical properties of conventional BCS theory have been intensively studied [23–29] with sometimes rather surprising insights [30, 31].

III. A TIGHT BINDING MODEL WITH JAHN-TELLER TYPE DISTORTION

As an illustrative example, we now augment the CuO_2 -model from section I by a Jahn-Teller type distortion. In particular, we will show how such distortions give rise to attractive $\mathbf{k}\mathbf{k}$ interactions sufficient for the occurrence of BCS states with such pairings. Our example of a lattice distortion is again intended to be a simplification of the possible dynamically induced and thus usually localized distortions. Consequently also many choices below will be made with simplicity and transparency of the resulting model in mind.

We begin by statically distorting the two oxygens of each unit cell away from their symmetric equilibrium positions to $r_{\text{O}(1)} = (a/2 + \delta_x, 0)$ and $r_{\text{O}(2)} = (0, a/2 + \delta_y)$. Here we adopt dimensionless units with lattice spacing $a = 1$. The distortion length parameters $\delta_x = \delta_y =: \delta$ are taken to be equal and small compared to the lattice constant a . This geometry is shown in Figure 2.

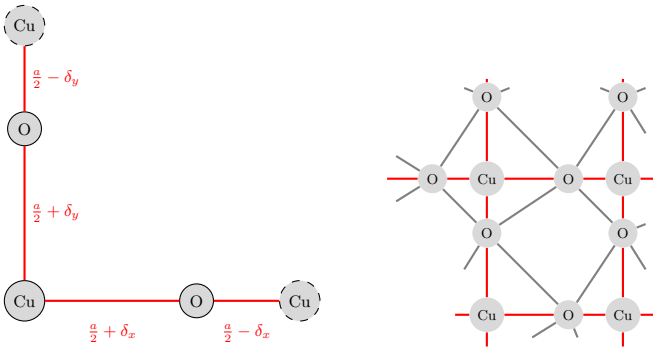


FIG. 2: An example of a Jahn-Teller type distortion to CuO_2 . On the left, a unit cell with displacements $\delta_{x/y}$ from the positions of the Oxygen atoms at the symmetry points $(a/2, 0)$ and $(0, a/2)$ along the respective axes is shown. On the right, the resulting deformed lattice and bond structure is indicated.

Firstly we calculate the electron-phonon coupling $D_\lambda(\mathbf{k})$ using a tight-binding wave function

$$\psi_{n,\mathbf{k}}(\mathbf{r}) = \frac{1}{\sqrt{N}} \sum_{j,\tau} c_{\tau,\mathbf{k}}^n e^{i\mathbf{k}\cdot\mathbf{R}_j} w_\tau(\mathbf{r} - \mathbf{R}_{j\tau}), \quad (13)$$

where $N = 3N_{\text{cell}}$ denotes the number of lattice ions. The coefficients $c_{\tau,\mathbf{k}}^n$ are the n -th eigenvector of a hopping Hamiltonian in the atomic basis

$$\mathcal{H} = \begin{pmatrix} \varepsilon_{\text{Cu}} & a_x & a_y \\ a_x^* & \varepsilon_{\text{O}_x} & c \\ a_y^* & c^* & \varepsilon_{\text{O}_y} \end{pmatrix} \quad (14)$$

modeled after the lattice structure from Figure 1, with $a_x := t_1 + t_1 e^{-ik_x}$, $a_y := t_1 + t_1 e^{-ik_y}$ and $c := t_2 + t_2 e^{ik_x} + t_2 e^{-ik_y} + t_2 e^{ik_x - ik_y}$. The parameter t_1 corresponds to horizontal and vertical Cu-O hopping, while t_2 is the amplitude for diagonal O-O hopping. Typical values in t_1 -units are $\varepsilon_{\text{Cu}} - \varepsilon_{\text{O}} \approx 2.5$ to $3.5 t_1$, while $t_2 \approx 0.5$ to $0.6 t_1$, with $t_1 \approx 1.2$ to 1.5 eV [32, 33]. Here we take $t_1 = 1.5$ eV, $t_2 = 0.6 t_1$, $\varepsilon_{\text{Cu}} = 4.5$ eV, while setting the oxygen ground state energy ε_{O} to zero by a redefinition of the Fermi energy. The resulting dispersion relation has three branches and is shown in Figure 3.

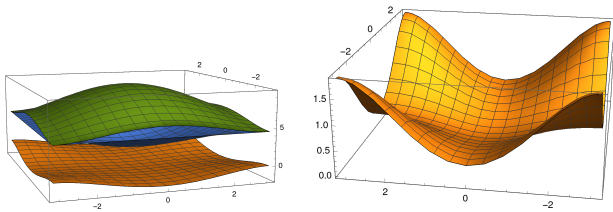


FIG. 3: Dispersion relation in the tight-binding model with $t_1 = 1.5$ eV, $t_2 = 0.825$ eV. For the BCS model we consider only the lowest branch (right).

For the atomic wave functions we take Gaussians $w_\tau(\mathbf{r}) := \mathcal{N}_\rho e^{-r^2/(4\rho^2)}$, with width ρ independent of

the atomic species τ and normalization $\mathcal{N}_\rho^{-1} = \sqrt{2\pi\rho^2}$. With this setup the resulting lattice-periodic wave functions are

$$u_{n,\mathbf{k}}(\mathbf{r}) = (2\pi)^2 \sum_{\tau} c_{\tau,\mathbf{k}}^n \sum_{\mathbf{G} \in \text{RL}} e^{-i\mathbf{r}\cdot\mathbf{G}} \hat{w}(\mathbf{k} - \mathbf{G}) e^{-i\mathbf{R}_\tau \cdot (\mathbf{k} - \mathbf{G})} \quad (15)$$

where the integral from the Fourier representation $w(\mathbf{r}) := \int d^2q e^{i\mathbf{r}\cdot\mathbf{q}} \hat{w}(\mathbf{q})$ of the atomic wave functions has already been carried out in combination with the lattice summation over j . The reciprocal lattice (RL) sum can be performed numerically with an appropriate truncation or analytically using special functions. Proceeding to the electron-phonon and induced electron-electron interactions (6), we consider here only the leading contributions from the smallest non-zero reciprocal lattice components $\tilde{\mathbf{G}} = (\pm 2\pi, 0)$, $(0, \pm 2\pi)$. For simplicity we will assume that electron-ion potential to be equal at these momenta and independent of τ . Thus abbreviating $v := \hat{v}_{\text{ei}}^\tau(\pm 2\pi, 0)$ we obtain

$$\begin{aligned} D_\lambda(\mathbf{k}) &\approx 2iv \sqrt{\frac{\hbar N_{\text{cell}}^3}{2\omega_\lambda(\mathbf{0})\Omega^4}} \left(\sum_{\tau} \frac{\mathbf{e}_{\lambda,\tau}(\mathbf{0})}{\sqrt{M_\tau}} \right) \cdot \left(\frac{2\pi I_{\mathbf{k}}^a(2\pi, 0)}{2\pi I_{\mathbf{k}}^a(0, 2\pi)} \right) \\ &= iv \sqrt{\frac{8\pi^2 \hbar}{\omega_\lambda(\mathbf{0})\Omega}} \mathbf{P}_\lambda \cdot \begin{pmatrix} I_{\mathbf{k}}^a(2\pi, 0) \\ I_{\mathbf{k}}^a(0, 2\pi) \end{pmatrix}, \end{aligned} \quad (16)$$

canceling $\Omega = a^2 N_{\text{cell}}$ and recalling that we use natural units with $a = 1$. In the second equality we prepare for carrying out the mode sum over λ in the effective electron-electron interaction (5) by introducing the polarization sum $\mathbf{P}_\lambda := \sum_{\tau} M_\tau^{-1/2} \mathbf{e}_{\lambda,\tau}(\mathbf{0})$. Further note that the first equality we already replaced the reciprocal lattice sum over the electronic integral from (6) restricted to $\tilde{\mathbf{G}} = (\pm 2\pi, 0)$, $(0, \pm 2\pi)$ by twice the anti-symmetric part

$$I_{\mathbf{k}}^a(\tilde{\mathbf{G}}) = i \int_{\text{cell}} d^2r \sin(\tilde{\mathbf{G}} \cdot \mathbf{r}) |u_{n,\mathbf{k}}(\mathbf{r})|^2 \quad (17)$$

with $\tilde{\mathbf{G}} = (2\pi, 0)$, $(0, 2\pi)$, as explained in more detail at the end of the appendix.

Guided by (5) we consider the two optical phonon modes with lowest energy. We denote their degenerate zero-momentum energy by $\omega_{10} := \omega_\lambda(\mathbf{0})$. The above mode and atomic sum turns out to be independent of the choice of basis of the doubly degenerate polarization space. Further, using standard methods [35] to analyze the phononic structure of the present model, a basis of polarizations can be chosen with non-zero components purely in the x - or y -coordinate direction, respectively, yielding polarization sums $\mathbf{P}_\lambda = (p, 0)$ or $(0, p)$ for the respective phonon modes λ for some constant $p \neq 0$. Our interpretation of the $\mathbf{k}\mathbf{k}$ pairs as an approximation of pairings with small relative momenta give an additional factor proportional to the volume Ω , as explained in the introduction. Any overall scale factors arising here are understood to be absorbed into the effective interaction constant v .

Altogether this yields a contribution to the effective electron-electron potential of

$$V(\mathbf{k}) \approx -\frac{8\pi^2\hbar|pv|^2}{\omega_{\text{lo}}^2} \left(|I_{\mathbf{k}}^a(2\pi, 0)|^2 + |I_{\mathbf{k}}^a(0, 2\pi)|^2 \right). \quad (18)$$

IV. RESULTS FOR THE GAP Δ AND PAIR-WAVE DENSITIES

We can now numerically demonstrate that the simplified distortion scheme from Figure 2 leads to a non-vanishing equal-momentum potential $V(\mathbf{k})$. In Figure 4 the result for distortion parameter $\delta = 0.05a$ is shown, with the remaining model parameters as in Section III. The atomic wave function width $\rho = 0.05a$ is chosen rather small for simplicity, as for larger widths overlaps of neighboring atomic wave functions are longer negligible if we require that (15) are well normalized. The numerics also confirm that $V(\mathbf{k})$ vanishes in the symmetric case with displacement $\delta = 0$, whereas $V < 0$ inside the first Brillouin zone if distortions are present.

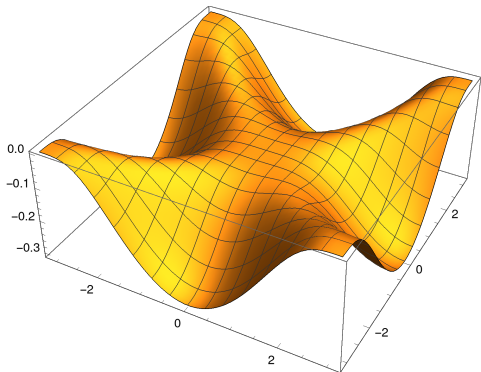


FIG. 4: The effective electron-electron potential V for the lowest electron branch in the first Brillouin zone, shown in units of $\hbar|pv|^2/\omega_{\text{lo}}^2$ for distortion parameter $\delta = \rho = 0.05a$.

Applying the results described in Section II, we obtain BCS states formed by $\mathbf{k}\mathbf{k}$ pairs for temperatures T below the critical temperature T^* . For this purpose we use the dispersion relation obtained as the lowest eigenvalue of the hopping Hamiltonian (14). The gap function $\Delta(\mathbf{k})$ can then be obtained directly from (9). For $T < T^*$ a non-vanishing gap starts to develop in the vicinity of the maxima of V on the Fermi surface and extends to a neighborhood of the full Fermi surface when lowering the temperature further as shown in Figure 5.

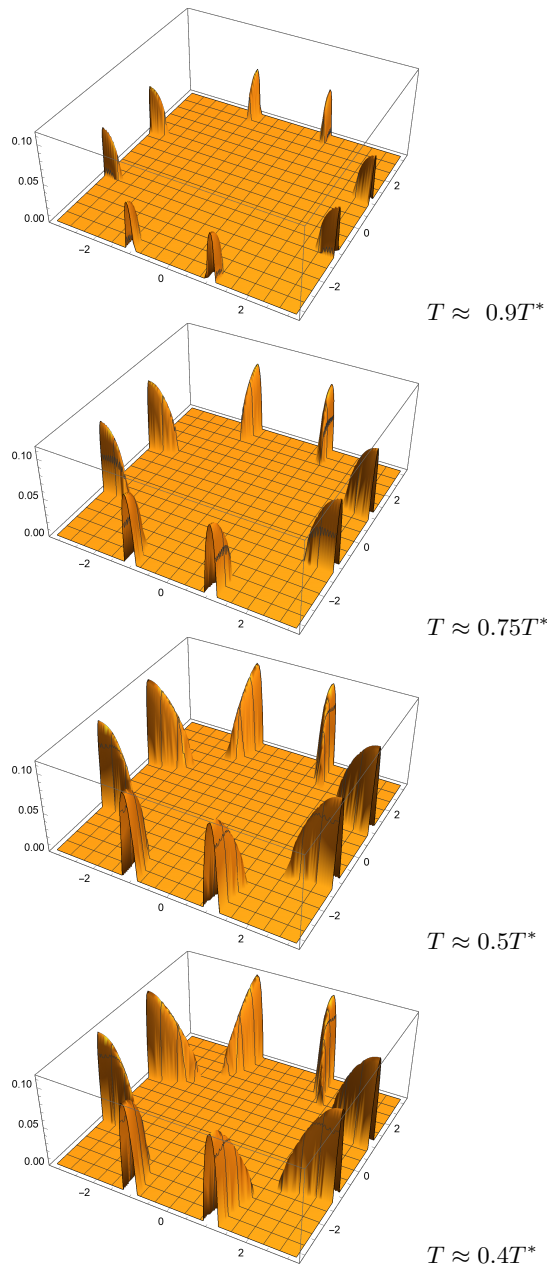


FIG. 5: The absolute value of the Gap function Δ in a tight-binding model with parameters $\rho = 0.05a$, $\delta = 0.05a$, $t_1 = 1.5$ eV, $t_2 = 0.85$ eV.

It should be recalled here that (9) yields only the absolute value $|\Delta(\mathbf{k})|$ of the gap function. On the other hand, the phase of the order parameter is not fixed by the present method, even to the extent that any choice of phase is consistent with this gap equation.

In Figures 6 and 7 we show the resulting pair density given by

$$\int_{\text{FBZ}} d^2k \alpha(\mathbf{k}) \cos(2\mathbf{k} \cdot \mathbf{r}) |u_{\mathbf{k}}(\mathbf{r})|^2, \quad (19)$$

with the pairing order $\alpha(\mathbf{k}) = \langle c_{\mathbf{k}\downarrow} c_{\mathbf{k}\uparrow} \rangle$ for two natural choices of the phase. In both cases, clear spatial modu-

lations of the pair density provide evidence for the emergence of pair density waves (PDW) in the present model.

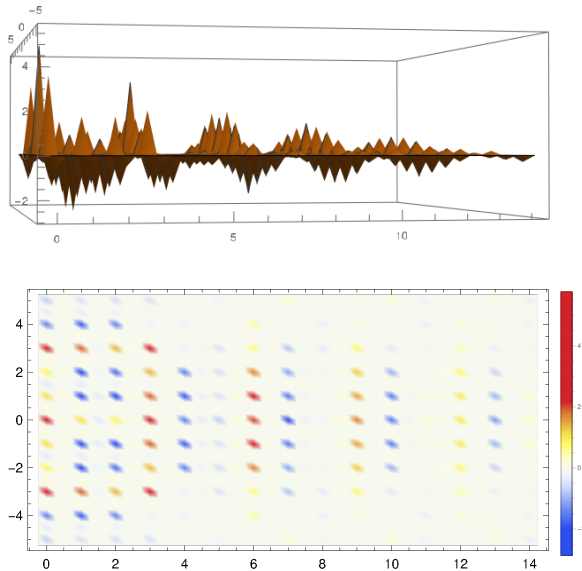


FIG. 6: Pair-wave density (19) in configuration space for order parameter $\alpha(\mathbf{k}) = |\alpha(\mathbf{k})|$ from Figure 5 at $T \approx 0.9T^*$, calculated via Riemann sums with $N = 101$ support points in both coordinate directions.

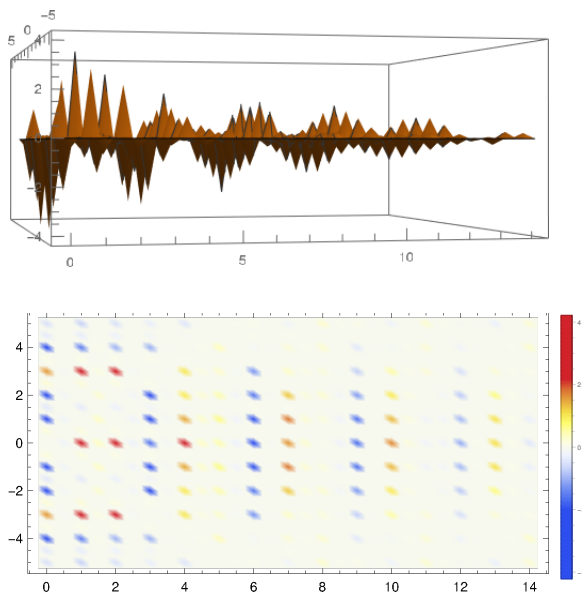


FIG. 7: Pair-wave density (19) with additional d-wave-like phase $\alpha(\mathbf{k}) = \sigma(\mathbf{k})|\alpha(\mathbf{k})|$ at $T \approx 0.9T^*$, $\sigma(\mathbf{k}) := \text{sgn}(k_x^2 - k_y^2)$.

Finally let us note that our model can easily be refined concerning various aspects. For example, one could take into account the influence of the distortion on the hopping parameters $t_{1(2)}$ or include contributions of higher-order reciprocal lattice components $\tilde{\mathbf{G}}$ in (16). Pursuing here would take us well beyond our present focus on the

salient features of the proposed pairing mechanism. We hope that such questions will be explored in subsequent works.

Conclusion

We investigate a novel BCS-type pairing mechanism in which electron-electron attraction is mediated by the interaction of low-momentum optical phonons and Jahn-Teller-type lattice distortions. To keep the model as simple as possible and allow for explicit calculations, we focus on the pairing of electrons with equal momenta. To demonstrate how this novel pairing mechanism can lead to instability of the Fermi sea, we consider a particular distortion of a planar CuO_2 lattice and using a tight-binding approximation, we numerically calculate the BCS gap function in this case. The resulting toy model exhibits the instability of the Fermi sea towards equal momentum pairing below a certain critical temperature T^* . Due to the simplicity of the approach, which also omits Coulomb interactions of electrons as well as density-density interactions and exchange energies, we expect T^* to represent not the actual critical temperature describing macroscopic coherence, but the existence of localized pairings such as the pseudogap. It is interesting to note that this appears to be the first microscopic model in which the pair density displays the characteristic features of a pair density wave (PDW).

Acknowledgement

C.H. is thankful to Mario Laux for his preliminary work on the model. C.H. also thanks Reinhold Kleiner and Niels Schopohl for fruitful discussions.

Appendix: Electron-Phonon Coupling in CuO_2

In order to get an expression for the electron-phonon potential, we follow the standard method outlined in many textbooks, e.g. [34, 35]. However, we take into account the effect of reciprocal lattice vectors and Umklapp processes since they play important part in our discussion of electron pairs with equal momenta.

Let Ω be the volume of a lattice with N_{cell} primitive cell, N_e electrons and let \mathbf{r} denotes the position of an electron. Using this notation, the electron-ion potential in the rigid ion approximation can be written as

$$V_{\text{el-ion}} = \sum_{l=1}^{N_e} \sum_{j=1}^{N_{\text{cell}}} \sum_{\tau} v_{\text{ei}}^{\tau}(\mathbf{r}_l - \mathbf{R}_{\tau j}), \quad (20)$$

where $\mathbf{R}_{\tau j}$ is the position of the “ τ ” atom in the “ j th” primitive cell and τ runs over the atomic basis. Note that

$V_{\text{el-ion}}$ is periodic in the lattice parameter. Our main assumption is that v_{ei}^τ is spin independent and has a Fourier representation such that

$$v_{\text{ei}}^\tau(\mathbf{r}) = \frac{1}{\Omega} \sum_{\mathbf{Q}} \hat{v}_{\text{ei}}^\tau(\mathbf{Q}) e^{i\mathbf{Q}\cdot\mathbf{r}}, \quad (21)$$

Note, that this assumption is fulfilled for example if v_{ei}^τ is periodic in the size of the lattice and bounded.

In second quantization notation, this potential can be written in terms of the creation (annihilation) operator $c_{n\mathbf{k}\sigma}^\dagger$ ($c_{n\mathbf{k}\sigma}$) of the one-particle electronic states characterized by the Bloch eigenstate $\psi_{n\mathbf{k}\sigma}$, with band index n , wave number k and spin σ , as follows

$$V_{\text{el-ion}} = \sum_{j,\tau} \sum_{\substack{n,m \\ \sigma}} \left\{ \int_{\Omega} d^2r \psi_{n\mathbf{k}'\sigma}^*(\mathbf{r}) v_{\text{ei}}^\tau(\mathbf{r} - \mathbf{R}_{\tau j}) \psi_{m\mathbf{k}\sigma}(\mathbf{r}) \right\} \cdot c_{n\mathbf{k}'\sigma}^\dagger c_{m\mathbf{k}\sigma}. \quad (22)$$

Taking into account the displacement of the ions from their equilibrium position, the ionic position can be written as

$$\mathbf{R}_{\tau j} = \mathbf{R}_{\tau j}^0 + \mathbf{u}(\mathbf{R}_{\tau j}^0), \quad (23)$$

where $\mathbf{R}_{\tau j}^0$ is the equilibrium position of the τj ion, while $\mathbf{u}_{\tau j}$ its displacement.

Now for small displacements, the potential can be expanded to first order as

$$v_{\text{ei}}^\tau(\mathbf{r} - \mathbf{R}_{\tau j}) = v_{\text{ei}}^\tau(\mathbf{r} - \mathbf{R}_{\tau j}^0) - \nabla_{\mathbf{r}} v_{\text{ei}}^\tau(\mathbf{r} - \mathbf{R}_{\tau j}^0) \cdot \mathbf{u}(\mathbf{R}_{\tau j}^0) + O(u^2). \quad (24)$$

Inserting this expansion in (22), the first term gives the ‘‘static’’ electron-ion interaction while the second is the electron-phonon interaction. Expressing the displacement of ions in terms of the phonon creation and annihilation operators $a_\lambda^\dagger(\mathbf{q})$, $a_\lambda(\mathbf{q})$, where λ is the branch index and \mathbf{q} is the phonon momentum taking values in the first Brillouin zone (FBZ), the electron-phonon interaction takes the form

$$V_{\text{el-ph}} = - \sum_{\mathbf{q} \in \text{FBZ}} \sum_{\substack{n,m \\ \lambda,\sigma}} \sum_{\mathbf{k}',\mathbf{k}} D_{\lambda,\sigma}^{nm}(\mathbf{k}',\mathbf{k},\mathbf{q}) \cdot c_{n\mathbf{k}'\sigma}^\dagger c_{m\mathbf{k}\sigma} (a_\lambda(\mathbf{q}) + a_\lambda^\dagger(-\mathbf{q})). \quad (25)$$

Where the electron-phonon coupling is given by

$$D_{\lambda,\sigma}^{nm}(\mathbf{k}',\mathbf{k},\mathbf{q}) = \sum_{j,\tau} \sqrt{\frac{\hbar}{2M_\tau N_{\text{cell}} \omega_\lambda(\mathbf{q})}} \mathbf{e}_{\lambda,\tau}(\mathbf{q}) e^{i\mathbf{q}\cdot\mathbf{R}_{\tau j}^0} \left\{ \int_{\Omega} d^2r \psi_{n\mathbf{k}'\sigma}^*(\mathbf{r}) \nabla_{\mathbf{r}} v_{\text{ei}}^\tau(\mathbf{r} - \mathbf{R}_{\tau j}^0) \psi_{m\mathbf{k}\sigma}(\mathbf{r}) \right\}. \quad (26)$$

Where $\mathbf{e}_{\lambda,\tau}(\mathbf{q})$ are the polarization vectors extracted from the eigenvector of the Dynamical matrix corresponding to eigenvalue $\omega_\lambda(\mathbf{q})$. Using that $\psi_{m\mathbf{k}\sigma}$ are Bloch

functions and summing over j , a simple calculation shows that the electron-phonon potential can be expressed in the terms of vectors in the reciprocal lattice (RL) as

$$V_{\text{el-ph}} = - \sum_{\substack{n,m,\lambda \\ \sigma}} \sum_{\mathbf{q} \in \text{FBZ}} \sum_{\substack{\mathbf{G} \in \text{RL} \\ \mathbf{k}+\mathbf{q}+\mathbf{G} \in \text{FBZ}}} D_{\lambda,\sigma}^{nm}(\mathbf{k},\mathbf{G},\mathbf{q}) \cdot c_{n\mathbf{k}+\mathbf{q}+\mathbf{G}\sigma}^\dagger c_{m\mathbf{k}\sigma} (a_\lambda(\mathbf{q}) + a_\lambda^\dagger(-\mathbf{q})), \quad (27)$$

where the coupling is now given by

$$D_{\lambda,\sigma}^{nm}(\mathbf{k},\mathbf{G},\mathbf{q}) = \sum_{\tau} \sqrt{\frac{\hbar N_{\text{cell}}}{2M_\tau \omega_\lambda(\mathbf{q})}} e^{-i\mathbf{G}\cdot\mathbf{R}_\tau^0} \mathbf{e}_{\lambda,\tau}(\mathbf{q}) \cdot \left\{ \int_{\Omega} d^2r \psi_{n\mathbf{k}+\mathbf{q}+\mathbf{G}\sigma}^*(\mathbf{r}) \nabla_{\mathbf{r}} v_{\text{ei}}^\tau(\mathbf{r}) \psi_{m\mathbf{k}\sigma}(\mathbf{r}) \right\}. \quad (28)$$

Using the Fourier representation of the electron-ion potential (21) and introducing the lattice periodic functions $u_{m\mathbf{k}\sigma}$ defined through $\psi_{m\mathbf{k}\sigma}(\mathbf{r}) = \frac{1}{\sqrt{\Omega}} e^{i\mathbf{k}\cdot\mathbf{r}} u_{m\mathbf{k}\sigma}$, the coupling now takes the form

$$D_{\lambda,\sigma}^{nm}(\mathbf{k},\mathbf{G},\mathbf{q}) = i \sum_{\tau,\mathbf{Q}} \frac{1}{\Omega^2} \sqrt{\frac{\hbar N_{\text{cell}}}{2M_\tau \omega_\lambda(\mathbf{q})}} e^{-i\mathbf{G}\cdot\mathbf{R}_\tau^0} \cdot (\mathbf{e}_{\lambda,\tau}(\mathbf{q}) \cdot \mathbf{Q}) \hat{v}_{\text{ei}}^\tau(\mathbf{Q}) \cdot \left\{ \int_{\Omega} d^2r e^{i\mathbf{Q}\cdot\mathbf{r}} e^{-i(\mathbf{q}+\mathbf{G})\cdot\mathbf{r}} u_{n\mathbf{k}+\mathbf{q}+\mathbf{G}\sigma}^*(\mathbf{r}) u_{m\mathbf{k}\sigma}(\mathbf{r}) \right\}. \quad (29)$$

Finally, since the functions $u_{m\mathbf{k}\sigma}$ are lattice periodic (with trivial spin dependence), the integral over the volume can be reduced to integrals over the primitive cells. Therefore,

$$D_{\lambda,\sigma}^{nm}(\mathbf{k},\mathbf{G},\mathbf{q}) = i \frac{N_{\text{cell}}}{\Omega^2} \sum_{\substack{\tau \\ \tilde{\mathbf{G}} \in \text{RL}}} \sqrt{\frac{\hbar N_{\text{cell}}}{2M_\tau \omega_\lambda(\mathbf{q})}} e^{-i\mathbf{G}\cdot\mathbf{R}_\tau^0} \cdot (\mathbf{e}_{\lambda,\tau}(\mathbf{q}) \cdot (\mathbf{q} + \mathbf{G} + \tilde{\mathbf{G}})) \hat{v}_{\text{ei}}^\tau(\mathbf{q} + \mathbf{G} + \tilde{\mathbf{G}}) \cdot \left\{ \int_{\text{cell}} d^2r e^{i\tilde{\mathbf{G}}\cdot\mathbf{r}} u_{n\mathbf{k}+\mathbf{q}+\mathbf{G}\sigma}^*(\mathbf{r}) u_{m\mathbf{k}\sigma}(\mathbf{r}) \right\}, \quad (30)$$

where the integral is now over the volume of the primitive cell.

Using the lowest order approximation of the Wegner flow [13, 14], one obtains the following effective electronic Hamiltonian

$$H_{\text{el}} = \sum_{\mathbf{k},n,\sigma} \varepsilon_n(\mathbf{k}) c_{n\mathbf{k}\sigma}^\dagger c_{n\mathbf{k}\sigma} + \sum_{\substack{\mathbf{k}n\sigma,\mathbf{k}'m\sigma' \\ \mathbf{q}n'm'\mathbf{G}\mathbf{G}'}} V_{\sigma\sigma'}^{nn'mm'}(\mathbf{k},\mathbf{k}',\mathbf{G},\mathbf{G}',\mathbf{q}) \cdot c_{n'\mathbf{k}+\mathbf{q}+\mathbf{G}\sigma'}^\dagger c_{m'\mathbf{k}'-\mathbf{q}+\mathbf{G}'\sigma'} c_{m\mathbf{k}\sigma} c_{n\mathbf{k}\sigma}, \quad (31)$$

where

$$V_{\sigma\sigma'}^{nn'mm'}(\mathbf{k}, \mathbf{k}', \mathbf{G}, \mathbf{G}', \mathbf{q}) = \sum_{\lambda} D_{\lambda\sigma'}^{mm'}(\mathbf{k}', \mathbf{G}', -\mathbf{q}) D_{\lambda\sigma}^{nn'}(\mathbf{k}, \mathbf{G}, \mathbf{q}) \cdot \frac{\beta_{\lambda nn'}(\mathbf{k}, \mathbf{G}, \mathbf{q}) - \alpha_{\lambda mm'}(\mathbf{k}', \mathbf{G}', -\mathbf{q})}{(\beta_{\lambda mm'}(\mathbf{k}', \mathbf{G}', -\mathbf{q}))^2 + (\alpha_{\lambda nn'}(\mathbf{k}, \mathbf{G}, \mathbf{q}))^2}, \quad (32)$$

$$\alpha_{\lambda mm'}(\mathbf{k}, \mathbf{G}, \mathbf{q}) = \varepsilon_{m'}(\mathbf{k} + \mathbf{q} + \mathbf{G}) - \varepsilon_m(\mathbf{k}) + \omega_{\lambda}(\mathbf{q}), \quad (33)$$

$$\beta_{\lambda mm'}(\mathbf{k}, \mathbf{G}, \mathbf{q}) = \varepsilon_{m'}(\mathbf{k} + \mathbf{q} + \mathbf{G}) - \varepsilon_m(\mathbf{k}) - \omega_{\lambda}(\mathbf{q}). \quad (34)$$

Eliminating the trivial spin dependence and restricting to a single band and optical phonon modes, for which $\omega_{\lambda}(0) \neq 0$, and defining $D_{\lambda}^n(\mathbf{k}) := D_{\lambda,\sigma}^{nn}(\mathbf{k}, \mathbf{0}, \mathbf{0})$ the electron-phonon coupling (30) yields the simple form (6), where we also dropped the band index for convenience.

Furthermore, using (6) along with (32), (33), (34) and setting $V(\mathbf{k}) = V_{\sigma\sigma'}^n(\mathbf{k}, \mathbf{k}, \mathbf{0}, \mathbf{0})$ one obtains the effective electron-electron interaction (5).

Now let's take a closer look at the electron-phonon coupling (6). Considering only the summation over $\tilde{\mathbf{G}} \in \text{RL}$ and assuming that the electron-ion potential v_{ei}^{τ} is real and reflection symmetric, which implies that its Fourier coefficients also satisfy $\hat{v}_{\text{ei}}^{\tau}(\tilde{\mathbf{G}}) = \hat{v}_{\text{ei}}^{\tau}(-\tilde{\mathbf{G}})$. Together with the scalar product $\mathbf{e}_{\lambda,\tau}(\mathbf{0}) \cdot \tilde{\mathbf{G}}$, we see that the prefactor of the electronic integral in (6) is anti-symmetric in $\tilde{\mathbf{G}}$. But this means that only the anti-symmetric parts of the electronic integrals

$$I_{\mathbf{k}}^a(\tilde{\mathbf{G}}) = i \int_{\text{cell}} d^3r \sin(\tilde{\mathbf{G}} \cdot \mathbf{r}) |u_{\mathbf{k}}(\mathbf{r})|^2 \quad (35)$$

can yield non-vanishing contributions to $D_{\lambda}(\mathbf{k})$. It is easy to see that in the case a ‘‘perfect’’ CuO_2 crystal, this integral vanishes. However, a Jahn-Teller type distortion, where the symmetry of the crystal is broken, can cause the integral (35) to be non-zero. Resulting in a non-zero electron-phonon coupling and the possible formation of equal momenta electron pairs.

-
- [1] A. Lanzara et al., *Nature* **412**, 510 (2001).
[2] G.-H. Gweon, S.Y. Zhou, M.C. Watson, T. Sasagawa, H. Takagi and A. Lanzara, *Phys. Rev. Lett.* **97**, 227001 (2006).
[3] Y. He et al., *Science* **362**, 62 (2018).
[4] J.J. Lee et al., *Nature* **515**, 245 (2014).
[5] S.-L. Yang, J. A. Sobota, Y. He, D. Leuenberger, H. Soifer, H. Eisaki, P. S. Kirchmann and Z.-X. Shen, *Phys. Rev. Lett.* **122**, 176403 (2019).
[6] T. P. Devereaux, T. Cuk, Z.-X. Shen and N. Nagaosa, *Phys. Rev. Lett.* **93**, 117004 (2004).
[7] J. G. Bednorz and K. A. Müller, *Zeitschrift für Physik B* **64**, 189 (1986).
[8] K. A. Müller, in *Magnetic Resonance and Relaxation*, R. Blinc, Ed., 192–208 (1966).
[9] K.-H. Höck, H. Nickisch, and H. Thomas, *Helvetica Phys. Acta* **56**, 237 (1983).
[10] H. Keller, A. Bussmann-Holder and K. A. Müller, *Materials Today* **11** 38 (2008).
[11] H. Keller and A. Bussmann-Holder, *Advances in Condensed Matter Physics* **2010**, 393526 (2010).
[12] C. Hainzl and M. Loss, *Eur. Phys. J. B* **90**, 82 (2017).
[13] F. Wegner, *Ann. Phys.* **506**,77 (1994).
[14] P. Lenz and F. Wegner, *Nucl. Phys. B* **482**, 693 (1996).
[15] H. Fröhlich, *Proc. of R. Soc. London A* **215**, 291(1952).
[16] J. Bardeen and D. Pines, *Phys. Rev.* **99**, 1140 (1955).
[17] P. Fulde, R.A. Ferrell, *Phys. Rev.* **135**, A550 (1964)
[18] A.I. Larkin, Yu.N. Ovchinnikov, *Zh. Eksp. Teor. Fiz* **47**, 1136 (1964).
[19] A.I. Larkin, Yu. N. Ovchinnikov, *Sov. Phys. JETP*, **20**, 762 (1965).
[20] D. F. Agterberg et al., *Annu. Rev. Condens.Matter Phys.* **11**, 231(2020).
[21] WL. Tu and TK. Lee, *Sci Rep* **9**, 1719 (2019).
[22] G. Aperia, C. Di Castro, M. Grilli and J. Lorenzana, *Nucl. Phys. B* **744**, 277 (2006).
[23] C. Hainzl, E. Hamza, R. Seiringer and J.P. Solovej, *Commun. Math. Phys.***281**, 349 (2008).
[24] R.L. Frank, C. Hainzl, S. Naboko and R. Seiringer, *J. Geom. Anal.***17**, 559(2007).
[25] R. L. Frank, C. Hainzl, R. Seiringer and J. P. Solovej, *J. Amer. Math. Soc.* **25**, 667 (2012).
[26] C. Hainzl and R. Seiringer, *Phys.Rev. B* **77**, 184517 (2008).
[27] C. Hainzl and R. Seiringer, *J. Math. Phys.***57**, 021101 (2016).
[28] R. L. Frank, C. Hainzl and E. Langmann, *J. Spect. Theory.* **9**, 1005 (2019).
[29] A. Deuchert, C. Hainzl, M. Schaub, arXiv:2105.05623.
[30] R. L. Frank, C. Hainzl, B. Schlein and R. Seiringer, *Lett. Math. Phys.* **106**, 913 (2016).
[31] C. Hainzl and J. Seyrich, *Eur. Phys. J. B* **89**, 133 (2016).
[32] R. Photopoulos and R. Frésard, *Ann. Phys.* 1900177 (2019).
[33] X. Wang, L. De’ Medici and A. J. Millis, *Phys. Rev. B* **83**, 094501 (2011).
[34] F. Han, *Modern Course in the Quantum Theory of Solids*, World Scientific (2012).
[35] J. Sólyom, *Fundamentals of the Physics of Solids*, Vol. 1–3, Springer, (2007, 2009, 2010).